Catalysis Letters (2020) 150:2841–2849
https://doi.org/10.1007/s10562-020-03190-3

Au Nanoparticles Confined in SBA-15 as a Highly Efficient and Stable Catalyst for Hydrogenation of Quinoline to 1,2,3,4-Tetrahydroquinoline

Jianbo Zhao[1] · Haifeng Yuan[1] · Xiaomei Qin · Kuan Tian[1] · Yingfan Liu[1] · Chengzhen Wei[2] · Zhiqiang Zhang[1] · Liming Zhou[3] · Shaoming Fang[3]

Received: 14 February 2020 / Accepted: 16 March 2020 / Published online: 25 March 2020
© Springer Science+Business Media, LLC, part of Springer Nature 2020

Abstract

Au nanoparticles confined within the mesopores of the modified SBA-15 were obtained through adsorption-reduction method and firstly employed as chemoselective catalyst for quinoline hydrogenation. The effects of Au loadings, calcination temperature as well as structure of support on catalytic performances of Au catalysts were explored. The as-obtained 1.2%Au@SBA-15-500 catalyst exhibited high activity, excellent selectivity towards 1,2,3,4-tetrahydroquinoline and extraordinary sintering-resistant property as high as 800 °C, which is sharp contrast to the 1.3%Au/SiO_2-500 catalyst. It also showed good recyclability and versatility for quinoline derivatives. The observed properties were assigned to small-sized Au nanoparticles and mesopores of SBA-15. Our work provides a facile and promising approach to construct metal nanocatalysts with high catalytic performance by the use of mesoporous materials.

Graphic Abstract

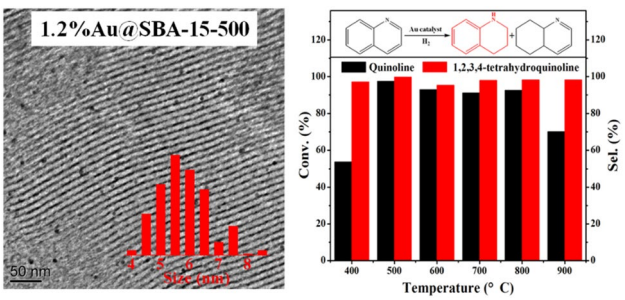

Keywords Au nanocatalyst · SBA-15 · Quinoline · Selective hydrogenation

✉ Jianbo Zhao
zhaojianbo@zzuli.edu.cn

✉ Liming Zhou
zlming1212@126.com

✉ Shaoming Fang
mingfang@zzuli.edu.cn

[1] School of Material and Chemical Engineering, Zhengzhou University of Light Industry, No. 136 of Science Road, Zhengzhou 450001, People's Republic of China

[2] Henan Province Key Laboratory of New Opto-Electronic Functional Materials, Anyang Normal University, Anyang, Henan 455000, People's Republic of China

[3] Henan Provincial Key Laboratory of Surface and Interface Science, Zhengzhou University of Light Industry, No. 136 of Science Road, Zhengzhou 450001, People's Republic of China

1 Introduction

N-heterocyclic compounds including 1,2,3,4-tetraquinoline have taken much interest because of their wide application in fine chemical fields such as dyes, agrochemicals and biological active molecules [1, 2]. Among the synthetic strategies to acquire 1,2,3,4-tetraquinoline, the quinoline hydrogenation is the most simple and powerful approach [3]. This kind of reaction was reported to proceed over homogeneous metal catalysts, such as Rh, Ru and Ir [4–7]. Unfortunately, these catalytic systems usually possessed some disadvantages such as the high cost of ligands and catalysts, rigorous reaction conditions, especially the difficulties in recovering the rare and expensive noble metal catalysts from the reaction mixtures [3]. From the standpoint of sustainable development, it is desirable that the reaction is carried out over heterogeneous catalysts under mild reaction conditions.

In recent years, heterogeneous metal nanocatalysts including Ru, Pd, Pt and Co have been developed for selective hydrogenation of quinoline compounds [8–15]. Many of them exhibited good catalytic properties, even so, the problem that often arises is that some catalytic systems were carried out at drastic reaction conditions (> 120 °C and/or 3.0 MPa H_2) [8, 13–15]. It is notable that the N-heterocyclic compounds typically act as poisons for these catalysts, which leads to the decrease and even loss of catalytic activity [9, 11]. Owing to good catalytic performances, especially extraordinary selectivity, heterogeneous gold catalysts have received more and more attention in selective hydrogenations [16–23]. Furthermore, quinoline compounds were found to be promoters and facilitate the activation of H_2 in the Au-catalyzed hydrogenation processes [22], which was in stark contrast with their poisoning action over traditional noble metal-based catalysts [9, 11, 22]. It is anticipated that the Au nanocatalysts can show the striking catalytic performance for hydrogenation of quinoline, but the research about it has been rarely reported [21, 22].

As an important class of mesoporous material, SBA-15 has the ordered adjustable channel size, high specific surface area and remarkable thermal stability, which provides an excellent support for the preparation of heterogeneous metal nanocatalysts [24–27]. For the above reasons, Au based catalysts deposited on SBA-15 were prepared and used in many transformations [26–30], however, to our best knowledge, no such research was found in the literature about them for selective hydrogenation of quinoline compounds. Herein, the Au nanocatalysts were synthesized using SBA-15 modified with APTES as a support and firstly employed for selective hydrogenation of quinoline. The effects of the gold loading, calcination temperature, specific surface area and porous structure of support on the performances of Au catalysts were studied in detail. High activity, excellent selectivity towards 1,2,3,4-tetrahydroquinoline and especially outstanding anti-sintering property were obtained over the as-prepared Au catalyst. Its performances were ascribed to the appropriate sizes of Au nanoparticles, high specific surface area and ordered mesopores of SBA-15.

2 Experimental

2.1 Raw Materials

SBA-15 was purchased from Nanjing XFNANO Materials Technology Company and chloroauric acid ($HAuCl_4 \cdot 3H_2O$, AR) was obtained from Shanghai Chemical Reagent Co., Ltd. 3-Amino-propyltrimethoxysilane (APTES) (≥ 98.0%, AR), quinoline (≥ 99.5%, AR) were provided from Sigma-Aldrich and Shanghai Macklin Biochemical Co., Ltd, respectively. $NaBH_4$ (≥ 99.0%, AR) was supplied from Sinopharm Chemical Reagent Co., Ltd. Other reagents were also analytical reagents.

2.2 Preparation of Au Nanocatalysts

The SBA-15 support was modification with APTES according to our previous procedure [31]. In a 100 mL three-necked flask, 1.8 g of APTES was added dropwise to 60 mL ethanol containing 1.0 g SBA-15 and the formed mixture was stirred at 90 °C for 24.0 h. Once being filtrated and washed, the resulting solid was dried at 60 °C for 10.0 h, denoted as SBA-15-APTES.

The Au@SBA-15 catalysts were constructed by the adsorption-reduction approach. Typically, 0.3 g SBA-15-APTES was mixed with 10 mL 0.003 mol L^{-1} $HAuCl_4$ aqueous solution under stirring. After 2.0 h, 1 mL cold deionized water consisting of 0.008 g $NaBH_4$ was added slowly to the aforementioned mixture and was stirred for 2.0 h. The solid sample was recovered, washed and dried under vacuum. Finally the pink Au catalyst was obtained after being calcined under a flow of air at 500 °C for 3 h, designated as 1.2%Au@SBA-15-500. Likewise, other SBA-15 supported Au catalysts were achieved by modify Au loadings or calcination temperature, denoted as X% Au@SBA-15-Y (X and Y represent the Au weight loading and calcination temperature, respectively). The SiO_2-supported Au catalysts as reference catalysts were also acquired according to the same procedure above.

2.3 Characterizations of Supports and Catalysts

The gold loadings were tested by Inductively Coupled Plasma Atomic Emission Spectrometry (ICP-AES) (Vista-MPX, Varian). N_2 adsorption–desorption isotherms were achieved from a Micromeritics Tristar 3000 instrument. The pore size distribution and the specific surface area were obtained using the BJH and BET methods, respectively. Power X-ray diffraction patterns (XRD) of samples were measured on a Shimadzu XRD-6000 using Cu Ka radiation operated at 40 kV and 30 mA. The TEM morphology and size distribution of Au catalysts were acquired using JEOL JEM-2100F transmission electron microscopy. X-ray photoelectron spectroscopy (XPS) was obtained under ultra-high vacuum ($< 10^{-6}$ Pa) on a Thermo Scientific ESCALAB 250Xi spectrometer with an Al anode (Al Kα = 1486.6 eV). All spectra were determined at room temperature and the binding energies (BE) were referred to 284.6 eV of the C 1 s peak.

2.4 Catalytic Hydrogenation Test

The quinoline hydrogenation was tested in a stainless steel autoclave under magnetic stirring. In a typical run, 3.0 mL of water, 60 μL of quinoline and 0.1 g of Au catalysts were added to the autoclave. After sealing, nitrogen was introduced to remove air for several times and pressurized with H_2 of 2.0 MPa. And then the reactor was heated to 100 °C and remained at this temperature under stirring. The reaction mixture was cooled and then extracted with ethyl acetate for 3 times when the reaction was completed. The resultant extract was measured by gas chromatography/mass spectrometry.

3 Results & Discussion

3.1 Physicochemical Properties of Catalysts

N_2 adsorption–desorption isotherms and pore size distribution curves of SBA-15 and corresponding Au catalysts were presented in Fig. 1, and their textural features and chemical compositions were listed Table 1. As seen from Fig. 1, with the exception of 1.3%Au/SiO_2, other samples displayed Langmuir type-IV isotherms with H1 hysteresis loop, possessing a feature of mesoporous materials [29, 32]. The specific surface area and pore size of Au catalysts decreased slightly with the increase of Au amounts. These results indicated that Au nanoparticles entered the mesopores of SBA-15, but the ordered mesoporous structure of SBA-15 remained unchanged.

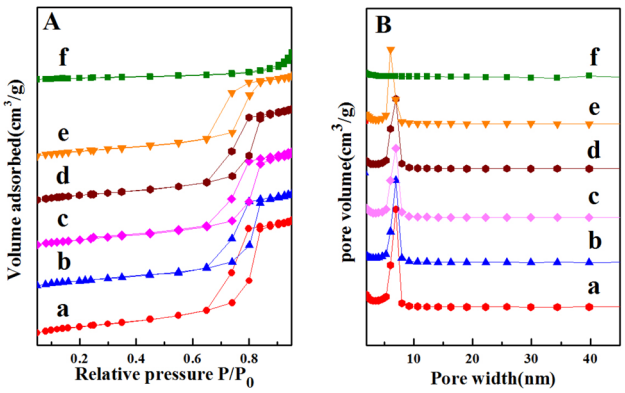

Fig. 1 N_2 adsorption–desorption isotherms (**A**) and BJH pore size distribution curves (**B**) of Au catalysts: (*a*) SBA-15, (*b*) 0.7%Au@SBA-15-500, (*c*) 1.2%Au@SBA-15-500, (*d*) 2.4%Au@SBA-15-500, (*e*) 1.2%Au@SBA-15-500 (used); (*f*) 1.3%Au/SiO_2-500

The XRD patterns of samples were showed in Fig. 2. The broad peak (2θ = 15°–30°) was ascribed to the amorphous silica [24, 29]. After gold nanoparticles were introduced, no apparent diffraction peaks assigned to Au were found on the resultant Au catalysts probably because of low Au loading and small-sized Au nanoparticles. It indicated the as-prepared Au catalysts remained almost the ordered structure of the SBA-15 host. The Au (111) diffraction peak of the 1.2%Au/SiO_2-800 catalyst was narrower compared with the 1.3%Au/SiO_2-500 catalyst, suggesting Au nanoparticles become larger after the calcination at 800 °C. Of note, the diameter of Au nanoparticles of Au catalysts cannot be correctly obtained from the XRD patterns because of the weak intensity of Au diffraction peaks. Their diameters can be measured by TEM images afterwards.

Figure 3 showed the FT-IR spectra of the samples. SBA-15 exhibited two absorption bands at 3127 and 1636 cm^{-1},which were related to stretching vibration ν(OH) and deformation vibration δ(OH) of Si–OH group, respectively. Besides, the other strong peak at 1092 cm^{-1} was assigned to stretching vibration ν(Si–O) of Si–OH group in Fig. 3a [31, 33]. After the SBA-15 support treated with APTES, these characteristic peaks of SBA-15 were retained, and the new peaks at 2923 and 1539 cm^{-1} associated with stretching vibration of CH_2 groups of pendant propyl chain and bending vibration of NH_2 groups were observed, respectively [30]. These results showed the APTES molecule was successfully grafted onto the surface of SBA-15. For the 1.2%Au@SBA-15-500 catalyst, the bending vibration of NH_2 group disappeared probably due to the calcination treatment [34]. The immobilization of Au nanoparticles on SBA-15-APTES can be confirmed by TEM and XPS characterizations

Table 1 Relevant physicochemical parameters of support and catalysts

Catalyst	Au content (wt%)	SBET (m^2g^{-1})	Vpore (cm^3g^{-1})	dpore (nm)
SBA-15	–	636.0	0.9	7.3
1%Au@SBA-15-500	0.7	598.7	0.8	6.9
2%Au@SBA-15-500	1.2	562.7	0.7	6.8
3%Au@SBA-15-500	2.4	547.8	0.6	6.7
2%Au@SBA-15-500(used)	1.2	554.9	0.7	6.6
2%Au/SiO_2-500	1.3	194.9	0.7	1.5

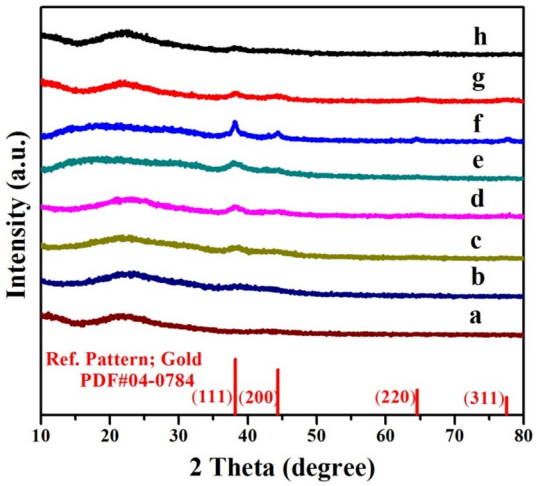

Fig. 2 XRD patterns of catalysts: (*a*) SBA-15; (*b*) 0.7%Au@SBA-15-500; (*c*) 1.2%Au@SBA-15-500; (*d*) 2.4%Au@SBA-15-500; (*e*) 1.3%Au/SiO_2-500; (*f*) 1.3%Au/SiO_2-800; (*g*) 1.2%Au@SBA-15-800; (*h*) 1.2%Au@SBA-15-500 (used)

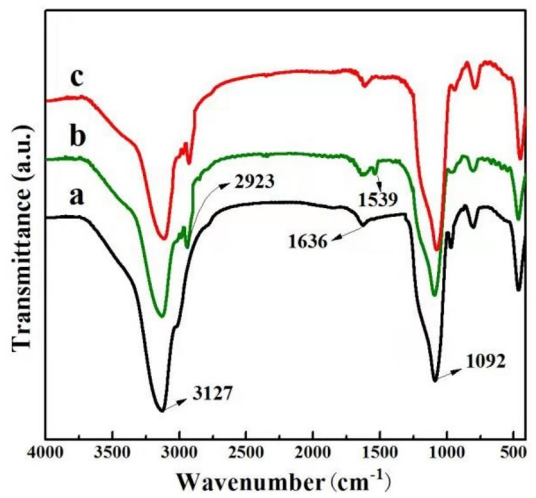

Fig. 3 FT-IR patterns of the samples: (*a*) SBA-15; (*b*) SBA-15 APTES; (*c*)1.2%Au@SBA-15-500

4 Micromorphology & Surface Property of Catalysts

Transmission electron microscopy (TEM) was conducted to obtain average sizes and size distributions of Au catalysts. It allowed us to follow how the size and structure of Au nanoparticles change according to the Au loading and calcination treatment. As seen from Fig. 4a–c, the spherical Au nanoparticles were dispersed within the mesopores of the SBA-15 support, and the mean diameters of Au nanoparticles of 0.7%Au@SBA-15-500, 1.2%Au@SBA-15-500 and 2.4%Au@SBA-15-500 increased from 3.3 ± 1.5 nm to 5.2 ± 0.6 nm and 5.6 ± 1.1 nm with the Au loadings, respectively. Of note, the Au nanoparticles of 1.2%Au@SBA-15–800 showed no significant change in spite of the calcination temperature up to 800 °C (Fig. 4d). It further confirmed that Au nanoparticles were located inside the mesopores of SBA-15. In contrast, 1.3%Au/SiO_2-500 as a reference catalyst possessed the comparable Au particle size with the wider distribution 5.8 ± 2.6 nm (Fig. 4e), while the Au nanoparticles located on the surface of SiO_2 agglomerated and increased sharply to 13.7 ± 6.3 nm after being calcined at 800 °C (Fig. 4f), which was also confirmed by XRD results. The chemical states of the as-synthesized Au catalysts were clarified by XPS (Fig. 4h). For 1.3%Au/SiO_2-500, 0.7%Au@SBA-15-500, 1.2%Au@SBA-15-500 and 2.4%Au@SBA-15-500, the binding energies of Au $4f_{7/2}$ were 83.7–83.8 eV, which were characteristic of $4f_{7/2}$ of the Au metallic [35, 36]. It indicated that Au existed in the state of Au^0 for the Au catalysts tested.

5 Catalytic Properties

The chemoselective hydrogenation of quinoline was employed to study the catalytic performances of Au nanocatalysts (Table 2). The plain SBA-15 support exhibited the poor catalytic activity, but the as-prepared Au catalysts delivered high activity and excellent selectivity under the

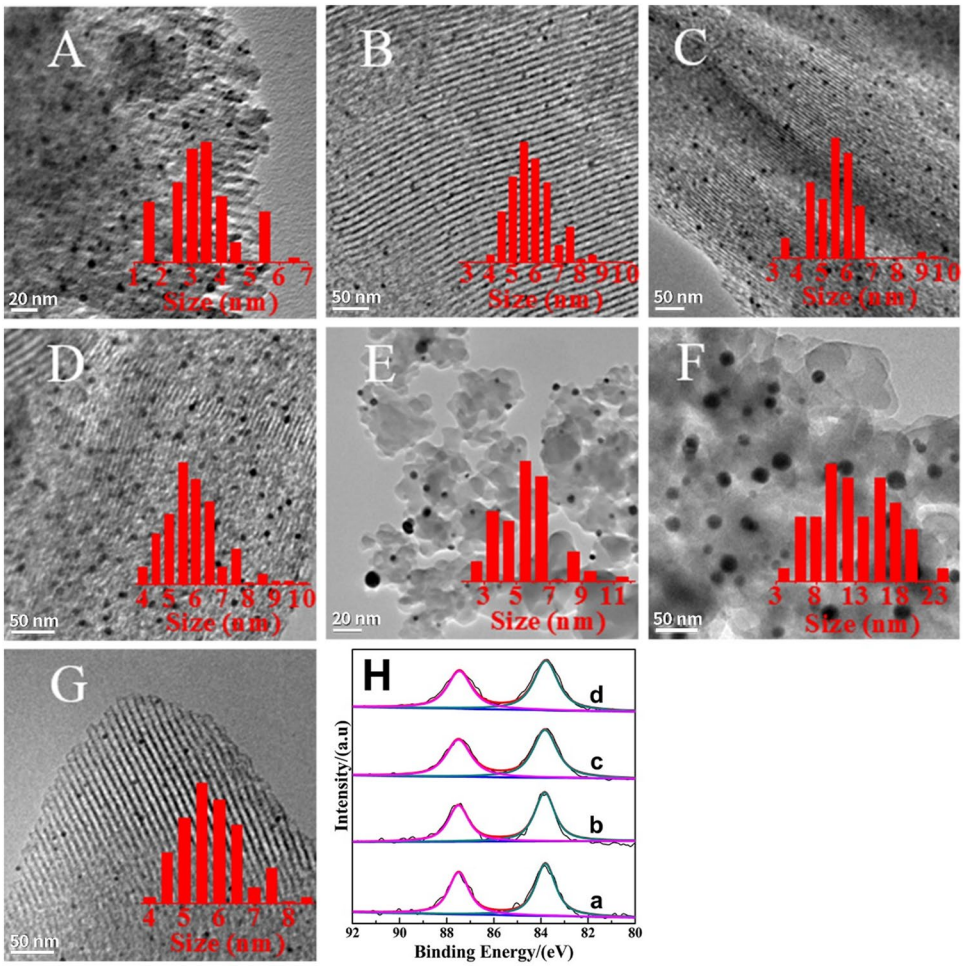

Fig. 4 Representative TEM images of Au catalysts: **A** 0.7%Au@SBA-15-500; **B** 1.2%Au@SBA-15-500; **C** 2.4%Au@SBA-15-500; **D** 1.2%Au@SBA-15-800; **E** 1.3%Au/SiO_2-500; **F** 1.3%Au@SiO_2-800; **G** 1.2%Au@SBA-15-500 (used); The insets show size distributions of Au nanoparticles. **H** Au 4f XPS spectra of typical Au catalysts: (*a*) 1.3%Au/SiO_2-500; (*b*) 0.7%Au@SBA-15-500; (*c*) 1.2%Au@SBA-15-500; (*d*) 2.4%Au@SBA-15-500

same reaction conditions. Combined with our XPS results, it showed that Au nanoparticles in the existence of metallic state is catalytic active sites, in also accordance with the previous report [37]. And then the influence of the Au loading was investigated. The 1.2%Au@SBA-15-500 catalyst showed the highest performances with 97.6% quinoline conversion and 99.8% selectivity towards 1,2,3,4-tetrahydroquinoline among observed gold catalysts (**Entry 2–4**). The adsorption and dissociation of hydrogen molecule is usually thought to be the rate-determining step in metal catalyzed-hydrogenation reactions [20, 21]. Small-sized Au nanoparticles have more low-coordinated edge and corner atoms, being considered to be catalytic active sites, and usually gave good activity. As shown in the results of XRD and TEM, the 0.7%Au@SBA-15 catalyst has the smallest size of Au nanoparticles. However, it exhibited lower activity than the 1.2%Au@SBA-15 catalyst. It indicates that an appropriate size of Au nanoparticles (about 5 nm) was required for selective hydrogenation of quinoline. The smaller Au nanoparticles do not necessarily mean the higher activity. This detailed reasons deserved to be explored in the future. The 1.2%Au@SBA-15-500 catalyst still delivered good activity and high selectivity of 1,2,3,4-tetrahydroquinoline when the reaction proceeded under the lower pressure of H_2 or at lower temperature (**Entry 5–7**). It showed that the 1.2% Au@SBA-15-500 was indeed a high performance catalyst for chemoselective hydrogenation of 1,2,3,4-quinoline.

The catalytic activity of Au nanocatalysts not only depends on the sizes of Au nanoparticles but also the type and structure of support [38, 39]. To elucidate the structure effect of support, 1.3%Au/SiO_2-500 was prepared with microporous SiO_2 as support and then employed in the selective hydrogenation of quinolone. Apparently, the 1.2%Au@SBA-15-500 catalyst showed higher activity than the 1.3%Au/SiO_2-500 catalyst (**Entry 3–8**). As shown in N_2 adsorption–desorption characterizations and TEM images above, due to the higher surface area of SBA-15, the Au nanoparticles of 1.2%Au@SBA-15-500 and 1.3%Au/SiO_2-500 had similar sizes, but the former showed a narrow size distribution. It in part accounted for the high activity of 1.2%Au@SBA-15-500. Besides, the ordered mesopore of SBA-15 made quinoline more accessible to the surface of Au nanoparticles, which also endowed 1.2%Au@SBA-15-500 with high activity. In the chemoselective hydrogenation of

Table 2 Selective hydrogenation of quinoline over different Au catalysts

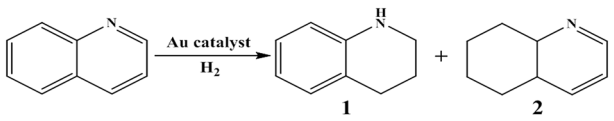

Entry	Cat	Conv./%[a]	Sel./%[a]	
			1	2
1	SBA-15	8.9	42.3	57.7
2	0.7%Au@SBA-15-500	51.3	92.3	7.7
3	1.2%Au@SBA-15-500	97.5	99.8	0.2
4	2.4%Au@SBA-15-500	96.2	98.7	1.3
5[b]	1.2%Au@SBA-15-500	91.1	98.7	1.4
6[c]	1.2%Au@SBA-15-500	73.6	97.3	2.7
7[d]	1.2%Au@SBA-15-500	86.2	98.1	1.9
8	1.3%Au/SiO_2-500	76.2	93.7	6.3

Reaction conditions: p(H_2) = 2.0 MPa; T = 100 °C; catalyst 0.1 g; quinoline 60 uL; water 3.0 mL; stirring speed = 500 r/min; reaction time 4 h

[a]The conversion of quinoline and selectivity towards 1,2,3,4-tetrahydroquinoline were determined by GC and GC–MS

[b]p(H_2) = 1.5 MPa

[c]p(H_2) = 1.0 MPa

[d]T = 80 °C

quinoline, the nitrogen-containing benzene ring preferred to adsorb on the surface of Au nanoparticles due to the interaction between Au and N, which is confirmed by the previous report [22]. And then the resulting hydrogen species, which originated from the adsorption and cleavage of H_2 over the surface of Au nanoparticles, interacted with the adsorbed quinoline and generated the 1,2,3,4-tetrahydroquinoline product. This configuration adsorption of quinoline over the surface of as-prepared Au catalysts led to the high selectivity towards 1,2,3,4-tetrahydroquinoline.

The effect of calcination temperature on the catalytic performances of Au catalysts was also explored. As seen from Fig. 5a, when the calcination temperature was 400 °C, the as-obtained Au catalysts showed the low activity. It was maybe related to the smaller size or chemical state of gold nanoparticles. While it increased to 500 °C, the 1.2%Au@SBA-15-800 catalyst afforded the quinoline conversion of 97.5% and selectivity towards 1,2,3,4-tetrahydroquinoline of 99.8%. It was worth nothing that the Au catalysts still possessed high activity even after being treated at 800 °C. The 92.5% quinoline conversion and 98.3% selectivity towards 1,2,3,4-tetraquinoline were obtained. It was ascribed to the similar mean sizes and size distribution of the 1.2%Au@SBA-15-500 and 1.2%Au@SBA-15-800 catalysts, which was confirmed by XRD and TEM results. To further elucidate the mechanism of outstanding anti-sintering property of the 1.2%Au@SBA-15-500 catalyst, the Au catalysts as a reference catalyst prepared from the same procedure with micropore SiO_2 as a support was employed in the hydrogenation of quinoline (Fig. 5b). The activity of the as-prepared Au catalyst firstly increased with the calcination temperature from 400 °C to 500 °C. The 1.3%Au/SiO_2-500 catalyst showed the good catalytic performance with 76.2% conversion of 1,2,3,4-quinoline and 93.7% selectivity towards 1,2,3,4-tarahydroquinoline. When the calcination temperature increased to 800 °C, the catalytic activity of the corresponding Au catalysts decreased drastically from 73.6%

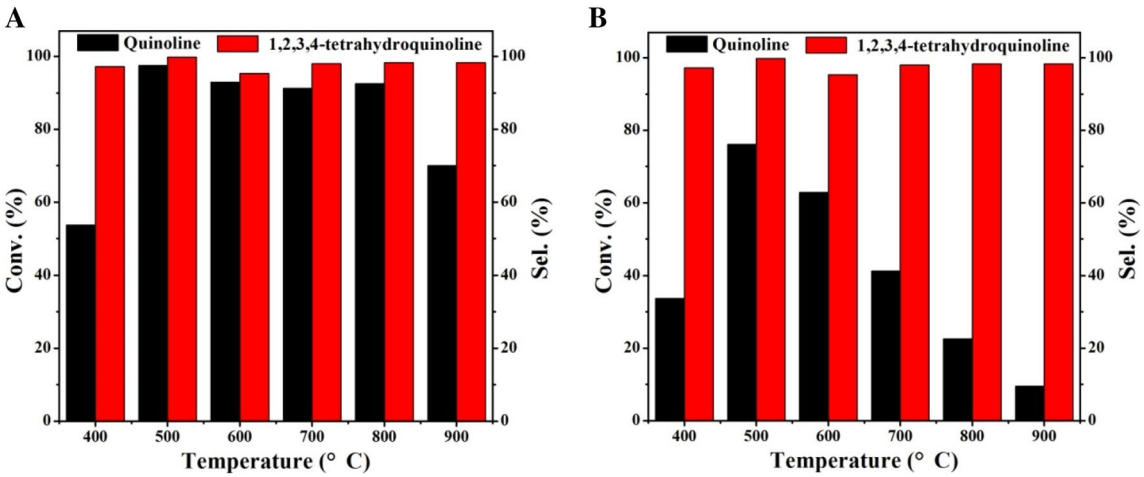

Fig. 5 The conversion and selectivity over **a** 1.2%Au@SBA-15 and **b** 1.3%Au/SiO_2 calcined at different temperatures. Reaction conditions: p(H_2) = 2.0 MPa; T = 100 °C; catalyst 0.1 g; quinoline 60 uL; water 3.0 mL; stirring speed = 500 r/min; reaction time 4 h. The conversion of quinoline and selectivity towards 1,2,3,4-tetrahydroquinoline were determined by GC and GC–MS

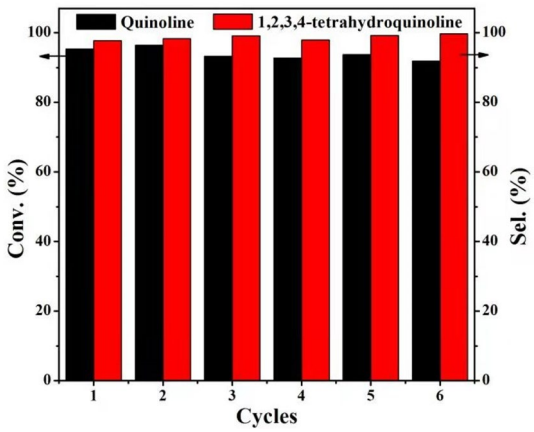

Fig. 6 Recyclability of 1.2% Au@SBA-15-500 for selective hydrogenation of quinoline. Reaction conditions: $p(H_2) = 2.0$ MPa; T = 100 °C; catalyst 0.1 g; quinoline 60 uL; water 3.0 mL; stirring speed = 500 r/min; reaction time 4 h

to 22.4%. According to the XRD and TEM results, the Au nanoparticles supported on SiO_2 sintered and agglomerated severely after the thermal treatment of 800 °C, resulting in the obvious loss in the activity of 1.3%Au/SiO_2-800. For the 1.2%Au@SBA-15-500 and 1.3%Au/SiO_2-500 catalysts, the dramatic difference in anti-sintering property should be associated with the structure of support. The confined effect of the ordered mesopore of SBA-15 can efficiently prevent the agglomeration of Au nanoparticles and so afford the as-prepared Au catalysts with extraordinary sintering-resistant property.

The reusability of 1.2%Au@SBA-15-500 catalyst was evaluated for the selective hydrogenation of quinoline. After the reaction ended, the 1.2%Au@SBA-15-500 catalyst was recovered by centrifugation, washed with ethyl acetate, dried and reused under the same reaction conditions. No significant decrease in activity and selectivity of 1.2%Au@SBA-15-500 was found when it was reused for 6 runs, as shown in Fig. 6. To disclose the mechanism of its good recyclability, the used 1.2%Au@SBA-15-500 catalyst was tested by series of characterizations. The Au amount of the catalyst after reaction from ICP-AES remained almost the same with that of the one before reaction. According to XRD (Fig. 2h) and TEM results (Fig. 4g), the average diameter and size distribution of Au particles of the used 1.2%Au@SBA-15-500 catalyst showed no obvious aggregation compared to the fresh one. Therefore, the 1.2%Au@SBA-15-500 catalyst was a stable and good recyclable catalyst for selective hydrogenation of quinoline.

The general applicability of the 1.2%Au@SBA-15-500 catalyst for chemoselective hydrogenation of quinoline derivatives was further explored. As found from Table 3, good to excellent conversions (91.1–100.0%) and high selectivities (78.7–100.0%) were obtained. It indicated that the 1.2%Au@SBA-15-500 catalysts was highly active and selective for hydrogenation reactions of quinoline compounds.

6 Conclusion

In conclusion, we reported the synthesis, characterizations of Au nanoparticles deposited on the modified SBA-15 support and the first use for the selective hydrogenation of quinoline. The 1.2%Au@SBA-15-500 catalyst afforded 97.6% conversion of quinoline and 99.8% selectivity towards 1,2,3,4-tetrahydroquinoline under mild conditions. It possessed outstanding sintering-resistant property as high as 800 °C, broad substrate scope and good reusability. The high specific surface area of SBA-15 and low Au loading contribute to small-sized gold nanoparticles, and ordered mesoporous of SBA-15 facilitate the mass transfer of substrates during the reaction, leading to high activity of gold nanocatalysts. This selective adsorption of the nitrogen-containing benzene ring on the surface of the Au catalysts accounted for the high selectivity towards 1,2,3,4-tetrahydroquinoline. The confinement of mesopores of SBA-15 can efficiently prevent gold nanoparticles from sintering at high temperature. It opens a promising avenue to construct metal nanocatalysts with high catalytic performance and especially outstanding anti-sintering property by the use of mesoporous materials.

Table 3 Selective hydrogenation of quinoline derivatives over 1.2%Au@SBA-15-500

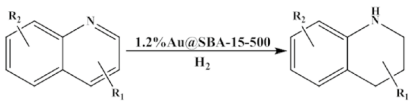

Entry	Substrate	Product	Conv. /%[a]	Sel. /%[a]
1	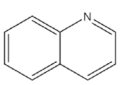	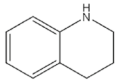	97.5	99.8
2	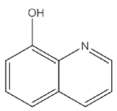	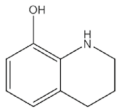	91.1	96.5
3	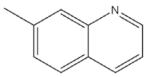	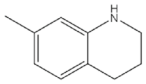	97.3	100.0
4	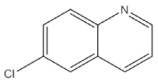	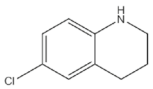	96.1	85.8[b]
5	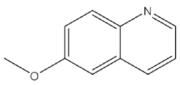	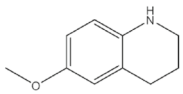	100.0	78.7[c]
6	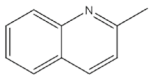	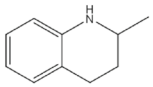	96.0	99.5

Reaction conditions: $p(H_2) = 2.0$ MPa; T = 100 °C; catalyst 0.1 g; quinoline 60 uL; water 3.0 mL; stirring speed = 500 r/min; reaction time 4 h

[a]The conv. of quinoline and sel. for the products were determined by GC and GC–MS

[b]6-Chloro-5,6,7,8-tetrahydroquinoline as the by-product were observed

[c]6-Methoxy-5,6,7,8-tetrahydroquinoline as the by-product were observed.

Acknowledgments This work was financially supported by the National Natural Science Foundation of China (Grant Nos. 21576248, 21671178 and 21571159) and a research fund from the doctoral program of Zhengzhou University of Light Industry (Grant No. 2014BSJJ007). The authors honestly thank Yongfa Zhu in Tsinghua University for good advices about XPS analysis.

Compliance with Ethical Standards

Conflict of interest The authors declare that they have no conflict of interest.

References

1. Shuman RT, Ornstein PL, Paschal JW, Gesellchen PD (1990) An improved synthesis of homoproline and derivatives. J Org Chem 55:738–741
2. Wang T, Zhuo LG, Li Z, Chen F, Ding Z, He Y, Fan QH, Xiang J, Yu ZX, Chan ASC (2011) Highly enantioselective hydrogenation of quinolines using phosphinefree chiral cationic ruthenium catalysts: scope, mechanism, and origin of Enantioselectivity. J Am Chem Soc 133:9878–9891
3. Gong Y, Zhang P, Xu X, Li Y, Li H, Wang Y (2013) A novel catalyst Pd@ompg-C_3N_4 for highly chemoselective hydrogenation of quinoline under mild conditions. J Catal 297:272–280
4. Alvarado Y, Busolo M, Lopez-Linares F (1999) Regioselective homogeneous hydrogenation of quinoline by use of pyrazolyl borate ligand and transition metal complexes as a precatalyst. J Mol Catal A-Chem 14:2163–2167
5. Kuwano R, Ikedaa R, Hirasadaa K (2015) Catalytic asymmetric hydrogenation of quinoline carbocycles: unusual chemoselectivity in the hydrogenation of quinolones. Chem Commun 51:7558–7561
6. Dobereiner GE, Nova A, Schley ND, Hazari N, Miller SJ, Eisenstein O, Crabtree RH (2011) Iridium-catalyzed hydrogenation of N-heterocyclic compounds under mild conditions by an outer-sphere pathway. J Am Chem Soc 133:7547–7562

7. Zhao D, Candish L, Paul D, Glorius F (2016) N-heterocyclic carbenes in asymmetric hydrogenation. ACS Catal 6:5978–5988
8. Sun YP, Fu HY, Zhang DL, Li RX, Chen H, Li XJ (2010) Complete hydrogenation of quinoline over hydroxyapatite supported ruthenium catalyst. Catal Commun 12:188–192
9. Konnerth H, Prechtl MHG (2017) Selective hydrogenation of N-heterocyclic compounds using Ru nanocatalysts in ionic liquids. Green Chem 19:2762–2767
10. Deraedt C, Ye R, Ralston WT, Toste FD, Somorjai GA (2017) Dendrimer-stabilized metal nanoparticles as efficient catalysts for reversible dehydrogenation/hydrogenation of N-heterocycles. J Am Chem Soc 139:18084–18092
11. Dell'Anna MM, Capodiferro VF, Mali M, Manno D, Cotugno P, Monopoli A, Mastrorilli P (2014) Highly selective hydrogenation of quinolines promoted by recyclable polymer supported palladium nanoparticles under mild conditions in aqueous medium. Appl Catal A-Gen 48:89–95
12. Zhang S, Xia Z, Ni T, Zhang Z, Ma Y, Qu Y (2018) Strong electronic metal-support interaction of Pt/CeO_2 enables efficient and selective hydrogenation of quinolines at room temperature. J Catal 359:101–111
13. Yu X, Nie R, Zhang H, Lu X, Zhou D, Xia Q (2018) Ordered mesoporous N-doped carbon supported Ru for selective adsorption and hydrogenation of quinoline. Micropor Mesopor Mat 256:10–17
14. Chen F, Surkus AE, He L, Pohl MM, Radnik J, Topf C, Junge K, Beller M (2015) Selective catalytic hydrogenation of heteroarenes with N-graphene-modified cobalt nanoparticles (Co_3O_4-Co/NGr@a-Al_2O_3). J Am Chem Soc 137:11718–11724
15. Wei Z, Chen Y, Wang J, Su D, Tang M, Mao S, Wang Y (2016) Cobalt encapsulated in N-doped graphene layers: an efficient and stable catalyst for hydrogenation of quinoline compounds. ACS Catal 6:5816–5822
16. Corma A, Serna P (2006) Chemoselective hydrogenation of nitro compounds with supported gold catalysts. Science 313:332–334
17. Liu C, Abroshan H, Yan C, Li G, Haruta M (2016) Ne-pot synthesis of $Au_{11}(PPh_2Py)_7Br_3$ for the highly chemoselective hydrogenation of nitrobenzaldehyde. ACS Catal 6:92–99
18. Zhao J, Jin R (2018) Heterogeneous catalysis by gold and gold-based bimetal nanoclusters. Nano Today 18:86–102
19. Zhao J, Li Q, Zhuang S, Song Y, Morris DJ, Zhou M, Wu Z, Zhang P, Jin R (2018) Reversible control of chemoselectivity in $Au_{38}(SR)_{24}$ nanocluster-catalyzed transfer hydrogenation of nitrobenzaldehyde derivatives. J Phys Chem Lett 9:7173–7179
20. Zhang L, Zhou M, Wang A, Zhang T (2020) Selective hydrogenation over supported metal catalysts: from nanoparticles to single atoms. Chem Rev 120:683–733
21. Zhao J, Ge L, Yuan H, Liu Y, Gui YH, Zhang B, Zhou L, Fang S (2019) Heterogeneous gold catalysts for selective hydrogenation: from nanoparticles to atomically precise nanoclusters. Nanoscale 11:11429–11436
22. Ren D, He L, Yu L, Ding RS, Liu YM, Cao Y, He HY, Fan KN (2012) An unusual chemoselective hydrogenation of quinoline compounds using supported gold catalysts. J Am Chem Soc 134:17592–17598
23. Tao L, Zhang Q, Li SS, Liu X, Liu YM, Cao Y (2015) Heterogeneous gold-catalyzed selective reductive transformation of quinolines with formic acid. Adv Synth Catal 357:753–760
24. Zhao D, Feng J, Huo Q, Melosh N, Fredrickson GH, Chmelka BF, Stucky GD (1998) Triblock copolymer syntheses of mesoporous silica with periodic 50 to 300 angstrom pores. Science 279:548–552
25. Xue Y, Yao R, Li J, Wang G, Wu P, Li X (2017) Efficient Pt-FeOx/TiO_2@SBA-15 catalysts for selective hydrogenation of cinnamaldehyde to cinnamyl alcohol. Catal Sci Technol 7:6112–6123
26. Li X, Fang SSS, Teo J, Foo YL, Borgna A, Lin M, Zhong Z (2012) Activation and deactivation of Au–Cu/SBA-15 catalyst for preferential oxidation of CO in H_2-rich gas. ACS Catal 2:360–369
27. Wang L, Meng X, Wang B, Chi W, Xiao FS (2010) Pyrrolidone-modified SBA-15 supported Au nanoparticles with superior catalytic properties in aerobic oxidation of alcohols. Chem Commun 46:5003–5005
28. Chen L, Hu J, Richards R (2009) Intercalation of aggregation-free and well-dispersed gold nanoparticles into the walls of mesoporous silica as a robust "green" catalyst for n-Alkane oxidation. J Am Chem Soc 131:914–915
29. Le NH, Hajjar-Garreau S, Bonne M, Megías-Sayago C, Louis B, Lebeau B, Balan L (2020) Photo-induced generation of size controlled Au nanoparticles on pure siliceous ordered mesoporous silica for catalytic applications. Micropor Mesopor Mat 295:109952
30. Masoud N, Delannoy L, Calers C, Gallet JJ, Bourn F, de Jong KP, Louis C, de Jongh PE (2017) Silica-supported Au–Ag catalysts for the selective hydrogenation of butadiene. ChemCatChem 9:2418–2425
31. Zhao J, Gui Y, Liu Y, Wang G, Zhang H, Sun Y, Fang S (2017) Highly efficient and magnetically recyclable Pt catalysts for hydrosilylation reactions. Catal Lett 147:1127–1132
32. Enumula SS, Koppadi KS, Gurram VRB, Burria DR, Kamaraju SRR (2017) Conversion of furfuryl alcohol to alkyl levulinate fuel additives over Al_2O_3/SBA-15 catalyst. Sustain Energy Fuels 1:644–651
33. Wang L, Kong A, Chen B, Ding H, Shan Y, He M (2005) Direct synthesis, characterization of Cu-SBA-15 and its high catalytic activity in hydroxylation of phenol by H_2O_2. J Mol Catal A Chem 230:143–150
34. Liu X, Wang A, Yang X, Zhang T, Mou CY, Su DS, Li J (2009) Synthesis of thermally stable and highly active bimetallic Au–Ag nanoparticles on inert supports. Chem Mater 21:410–418
35. Park ED, Lee JS (1999) Effects of pretreatment conditions on CO oxidation over supported Au catalysts. J Catal 186:1–11
36. Zhao J, Yu G, Xin K, Li L, Fu T, Cui Y, Liu H, Xue N, Peng L, Ding W (2014) Highly active gold catalysts loaded on NiAl-oxide derived from layered double hydroxide for aerobic alcohol oxidation. Appl Catal A-Gen 482:294–299
37. Boronat M, Illas F, Corma A (2009) Active sites for H_2 adsorption and activation in Au/TiO_2 and the role of the support. J Phys Chem A 113:3750–3757
38. Bore MT, Pham HN, Switzer EE, Ward TL, Fukuoka A, Datye AK (2005) The role of pore size and structure on the thermal stability of gold nanoparticles within mesoporous silica. J Phys Chem B 109:2873–2880
39. Wang S, Zhao Q, Wei H, Wang JQ, Cho M, Cho HS, Terasaki O, Wan Y (2013) Aggregation-free gold nanoparticles in ordered mesoporous carbons: toward highly active and stable heterogeneous catalysts. J Am Chem Soc 135:11849–11860

Publisher's Note Springer Nature remains neutral with regard to jurisdictional claims in published maps and institutional affiliations.